Penerbit Akademia Baru

Journal of Advanced Research in Fluid Mechanics and Thermal Sciences

Journal homepage: www.akademiabaru.com/arfmts.html
ISSN: 2289-7879

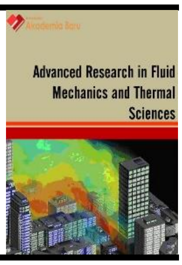

Development and Testing of Open-Jet Wind Tunnel for Quadrotor Flight Testing

Open Access

M. Z. Jurij[1], Elya Mohd Nor[1], Azmin Shakrine Mohd Rafie[2], Omar Faruqi Marzuki[2], Mohd Rashdan Saad[3], Syaril Azrad[2,*]

[1] Department of Electric and Electronic Engineering, Faculty of Engineering, Universiti Pertahanan Nasional Malaysia, Malaysia
[2] Department of Aerospace Engineering, Faculty of Engineering, Universiti Putra Malaysia, Malaysia
[3] Department of Mechanical Engineering, Faculty of Engineering, Universiti Pertahanan Nasional Malaysia, Malaysia

ARTICLE INFO

Article history:
Received 15 October 2019
Received in revised form 21 November 2019
Accepted 22 November 2019
Available online 28 December 2019

Keywords:
open-jet wind tunnel; wind distribution; wind speed; quadrotor testing; unmanned aerial vehicle

ABSTRACT

Station keeping of a hovering quadrotor under various turbulent wind condition has gained much attention these days due to its potential application in complex environments. Various types of control algorithm have been developed to increase the performance of the quadrotor under such wind conditions. These need to be tested and verified by flying the quadrotor itself. One of the quick and low-cost solutions would be to set up a test rig by modifying an existing wind tunnel to recreate such wind conditions. In order to cater such experiments, in Universiti Putra Malaysia (UPM), an open-jet wind tunnel was attached to an existing open-loop wind tunnel, which initially has a test area of 1 meter by 1-meter size. By attaching the open-jet wind tunnel which has a diverged shape, the test section area is increased up to 2 meters in diameter size, ensuring sufficient space for manoeuvring and hovering the experimental quadrotor. A settling chamber is attached before the test section to characterize the output wind. The maximum wind speed at the opening is 8 m/s. The extended wind tunnel's flow characteristics are analyzed by anemometer for velocity distribution in four different distance from the opening. It has been found that the wind velocity distribution and turbulent intensity simulate the outdoor wind turbulent condition to test a quadrotor hovering control algorithm.

1. Introduction

Multirotor unmanned aerial vehicles (UAVs) has become more practical for a wide range of applications not only in the normal and safe operating environment but in highly complex conditions such under highly speed wind and highly intense wind turbulent condition. It has been a daunting task to maneuver multirotor UAVs in such environment safely.

One important strategy to deal with turbulent wind conditions would be using robust control algorithm. In order to test the performance of the control strategy, one method is to use computer-

* *Corresponding author.*
E-mail address: syaril@upm.edu.my (Syaril Azrad)

based simulations. Several research groups have used this approach to simulate UAVs in turbulent conditions such as using ONERA simulation by Perozzi *et al.,* [1], using both computer simulation and outdoor tests by Ke *et al.,* [2] and Joyo *et al.,* [3] using MATLAB.

The other method is to implement the algorithm by conducting flight test in turbulent wind condition. In this method, the ability to repeatedly recreate wind turbulence that possesses a particular characteristic, pose a significant challenge to researchers. Waslander and Wang [4] works depend on the outdoor wind to study the effectiveness of their wind disturbance estimation and rejection strategy. Bannwarth *et al.,* [5] and Elya *et al.,* [6] applied a portable fan to generate wind disturbances indoors to study wind rejection.

Several control strategies for quadrotors to hover and navigate under turbulence condition have been developed and tested by Elya *et al.,* [7] in UPM and had shown excellent performance. However, further studies need to be done to relate between control parameters such as gain with the wind characteristics. The application wind tunnel will enable such studies to be done systematically due to its repeatability. Zain *et al.,* [8] conducted wind tunnel experiments to study the effect of active flow control applied on a sharped-edged generic delta-wing UAV and has shown good results attributed to the consistency of the wind characteristics that was generated. In order to enable quadrotor flight tests an open-jet wind tunnel is developed at Universiti Putra Malaysia by modifying an existing wind tunnel. The size and length of the open-jet wind tunnel are constricted by the space available in the Aerodynamic laboratory, as it is an extension of open-loop wind tunnel blower section. The open-jet wind tunnel is designed to output wind speed characterized by its speed and turbulence intensity. Similarly, Bannwarth *et al.,* [9] have designed a setup in wind tunnel for quadrotor flight testing under turbulence condition. However, as mentioned in their work, the setup has a limitation due to the usage of pre-existing equipment, and no modifications to the wind tunnel and the airflow conditioning grid were involved.

The designed open-jet wind tunnel also needs to take into account the relatively low wind speed condition of Malaysia, which has an average of 2 m/s to 3m/s according to the studies by Kamarudin *et al.,* [10] and Ahmadian *et al.,* [11]. This is because, initial verification and application from test results at the wind tunnel, the quadrotor will then have to be tested outdoor under local wind conditions.

In order to replicate the condition of the outdoor environment for future applications, the turbulent intensity of the test section also needs to be considered and conditioned accordingly. Analysis done by Ren *et al.,* [12] has shown that for onshore wind farms, the actual wind speed turbulence intensities are found below 20 %. It was also found that by Carpman [13], for a complex and uniform environment such as in an urban site and forest treetop with height less than 100 meters above the ground the wind turbulence intensity is almost 20%. The range of height in the study by Carpman is also the usual operating altitude quadrotor flight for normal applications. The outdoor wind turbulent intensity is also found around 20 % by Tabrizi *et al.,* [14], which used ultrasonic anemometers to measure above rooftop buildings for the study of small wind turbines. The configuration of street canyon in urban areas for modelling wind flow conditions and pollutant dispersions in the vortex formation studies conducted by Yazid *et al.,* [15] were taken as up to 20 meters high in average, which is significant for our case in studying the effect of wind turbulence on quadrotor flight.

It has been demonstrated by Vita *et al.,* [16] and Ahmadi-Baloutaki *et al.,* [17], that the usage of grids that can generate turbulence is considered as the most effective and reliable method to produce turbulent inflow for wind tunnel testing, and suitable for aerodynamic based research application, such as recreating wind flow in urban environment. Azzawi *et al.,* [18] show that by installing additional mesh screen and honeycomb as flow conditioning devices in the empty test section of their open-jet tunnel has succeeded to reduce turbulence intensity up to 33 %. They pointed out that further improvement in the prediction of the test section turbulent intensity can be achieved by modeling the mesh screen and honeycomb as a porous domain in Computational Fluid Dynamics.

This paper describes the modification of the existing UPM wind tunnel to enable flight testing of quadrotor UAV under turbulent winds and followed by the characterization of the flow quality measured from the turbulence intensity at different locations in the flow.

2. Methodology

The modified open-jet wind tunnel is designed based on the current subsonic wind tunnel available in the Aerodynamics Laboratory of UPM. The open-loop wind tunnel is modified by connecting a new extended diffuser to the downstream section of the wind tunnel, which acts as a second test section before the flow exits. Figure 1 shows the schematic diagram of the modified wind tunnel with the attachment of the extended diffuser. Multiple layers of wire mesh and honeycomb structures as listed in Table 1 are attached before the extended diffuser section to ensure the uniformity of the flow entering the second test section. Figure 2 shows the front side of the open-jet wind tunnel with a diameter of 2.3 m and the connection between the current open-loop wind tunnel exit and the new extension diffuser for the new open-jet wind tunnel.

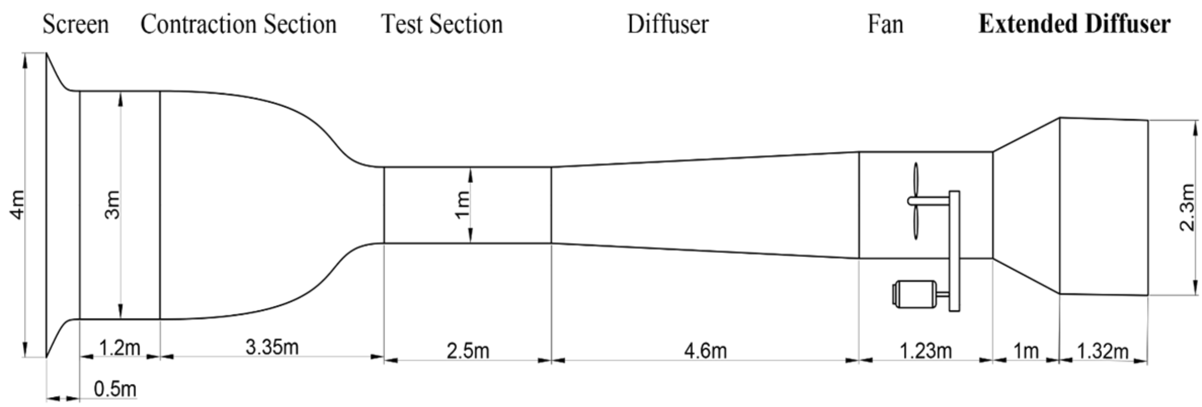

Fig. 1. Universiti Putra Malaysia open-loop wind tunnel specification [20]

Fig. 2. Open-jet wind tunnel outlet and attachment part for the extension of open-loop wind tunnel blower section

The equipment used for the measurement of wind speed distribution is an anemometer with Standard and Industrial Research Institute of Malaysia (SIRIM) calibrated. The anemometer is used to take readings at the pre-selected points on the open-jet wind tunnel outlet. Figure 3 shows the upstream view from the downstream location of the wind tunnel which "X" represent measurement point locations with a total of 53 distribution points. At each distribution points, six wind speed data measurements were conducted. Figure 4 is the top view of the wind tunnel showing the extension of the open-loop wind tunnel with four different measurement planes along the freestream flow direction. The experiments were done by gradually increasing the wind speed, and for every increment, the wind speed distribution is recorded. The distance of the measurement planes from the honeycomb structure (as a reference point) is as the followings; Position 1(0 cm), Position 2 (42.5 cm), Position 3 (85 cm) and Position 4 (127.5 cm).

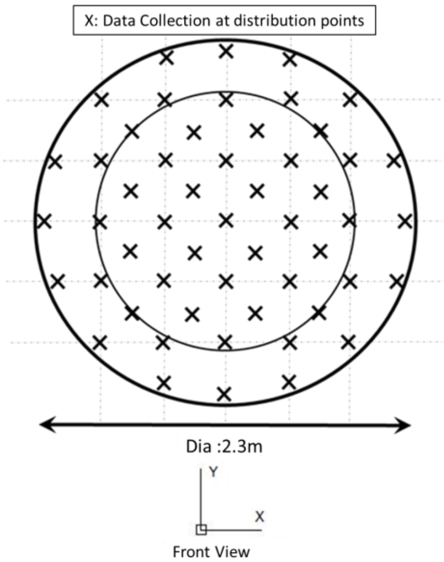

Fig. 3. Attachment front view, as "X" represent wind data distribution point locations

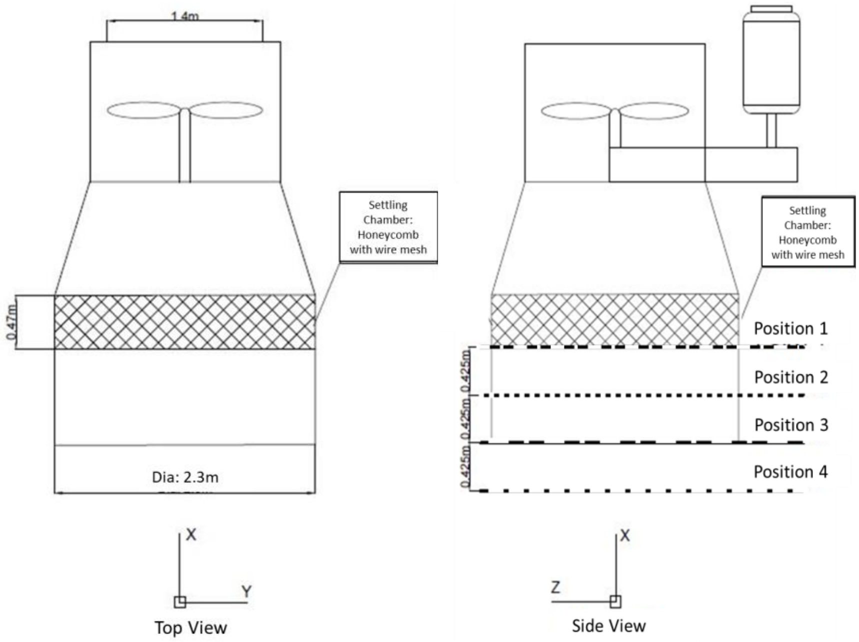

Fig. 4. Attachment top view and side-view with Position 1,2,3,4 locations

Table 1
Settling chamber specifications and grid shapes, starting from Layer 1 near to open-jet wind tunnel outlet and all layers are attached to each other

Grid shape/ Description	Diameter Shape (cm)	Thickness (cm)
Layer 1 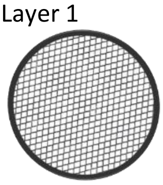	4	0.5
Layer 2 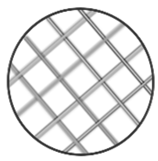	46	30
Layer 3 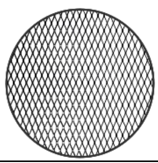	0.5	0.5

For the Motion Capture system that intended to be employed in the UAV tracking study, the minimum requirement is a 4-unit Optitrack low-cost camera system, mounted on a stand located at the downstream of the wind tunnel outlet as shown in Figure 5. Due to lab space constraints, a 2-unit barricade is used to block the second test section from outdoor sunlight and external free-stream wind. Besides their low costs, the Optitrack cameras do not require a fixed location which is an advantage to our applications. The cameras can be mounted at any position and be calibrated to the software of the system. The quadrotor that will be tested later will be applying open-source controller platform as being reviewed by Sabikan *et al.,* [19].

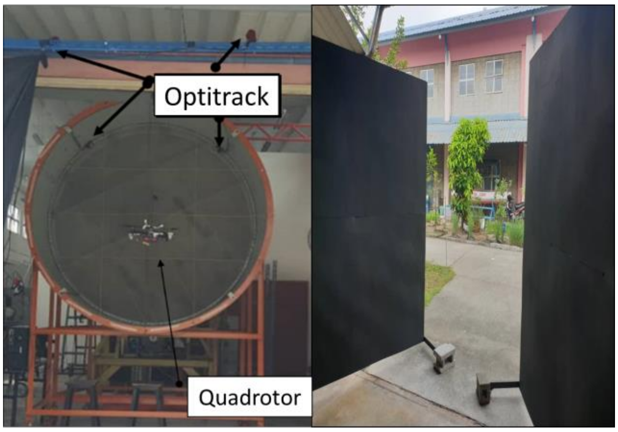

Fig. 5. Motion capture with 4 Optitrack cameras with Quadrotor as the test subject and black barricade

3. Results

Measurements are made at several wind distribution points by anemometer shown in Figure 4. The results of wind speed and turbulence intensity are tabulated in Table 2. We found that the wind speed at the tunnel opening increased linearly with the increment of the wind tunnel motor frequency, as shown graphically in Figure 6. It is also found that the maximum wind speed capability for the open-jet wind tunnel configured shown in Figure 4 is 8.9 m/s. This is due to the open-loop wind tunnel blower limitation. The overall results from Table 2 show that the turbulence intensity varies in the range between 17 % up to 24 % as the wind speed increases. This means the wind generated from the extended diffuser is laminar flow with several percentages of turbulence intensity as the wind speed increases.

Table 2
Open-jet wind tunnel wind speed measured at Position 1 (Figure 4)

Wind tunnel motor frequency (Hz)	Wind speed average (m/s)	Standard deviation	Turbulence Intensity (%)
0	0	0	0
5	0.64	0.28	43.95
10	1.96	0.34	17.33
15	3.02	0.53	17.63
20	4.24	0.72	17.04
24	4.94	1.13	22.83
25	5.16	0.88	17.05
27	5.74	1.22	21.20
34	7.30	1.56	21.38
37	7.77	1.86	23.90
40	8.90	2.44	27.35

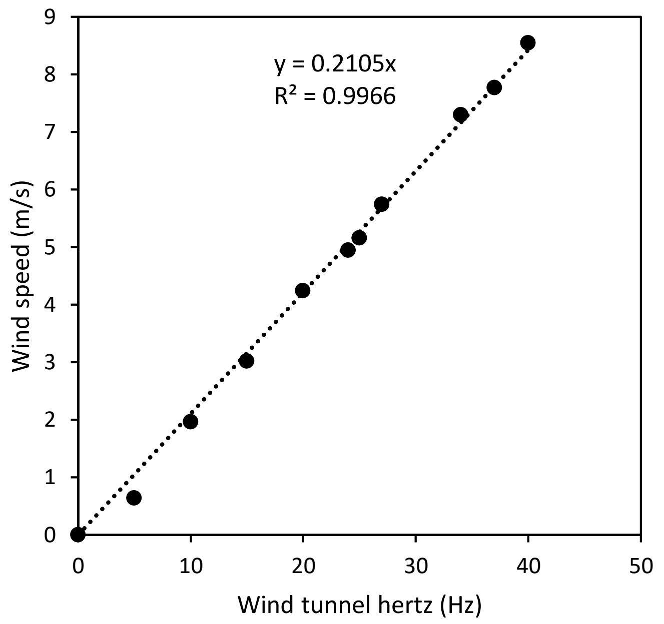

Fig. 6. Open-jet wind tunnel wind speed versus wind tunnel motor frequency (Hz)

Figure 7 shows the wind speed boundary layer at the outlet of the wind tunnel at Position 1,2, 3 and 4. The measurement points of wind speeds are taken at the centerline of the wind tunnel in the y-axis, as shown in Figure 8. In this result, the wind tunnel motor frequency was set at a maximum which is 40 Hz, that produced the highest wind speed of the wind tunnel.

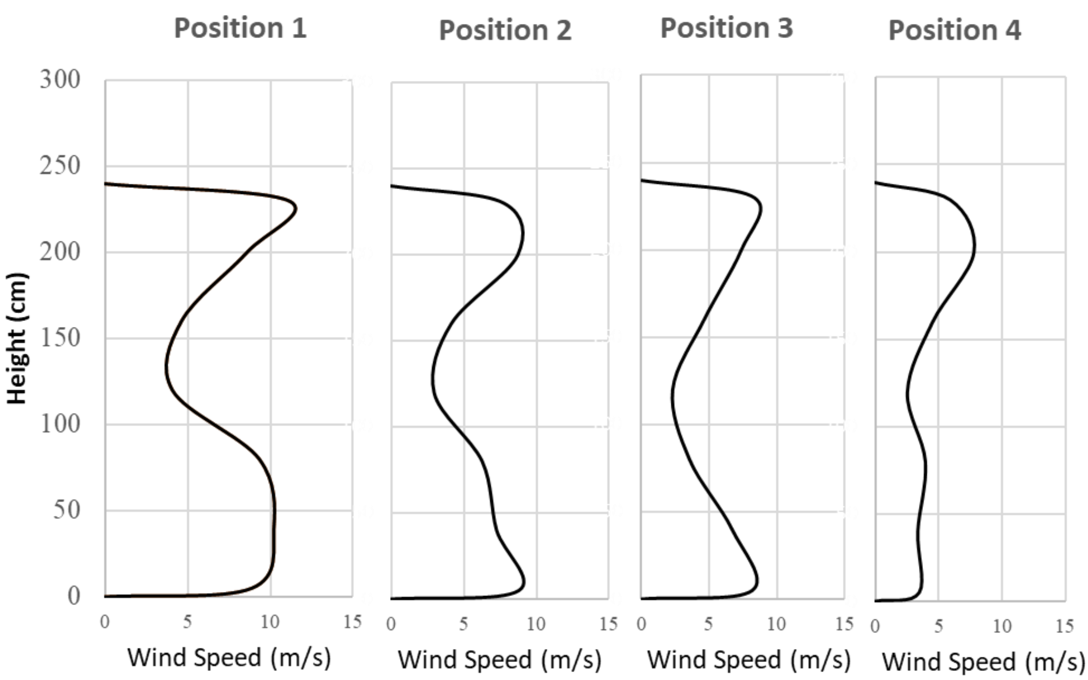

Fig. 7. Wind speed vs. height at center line Wind boundary profile

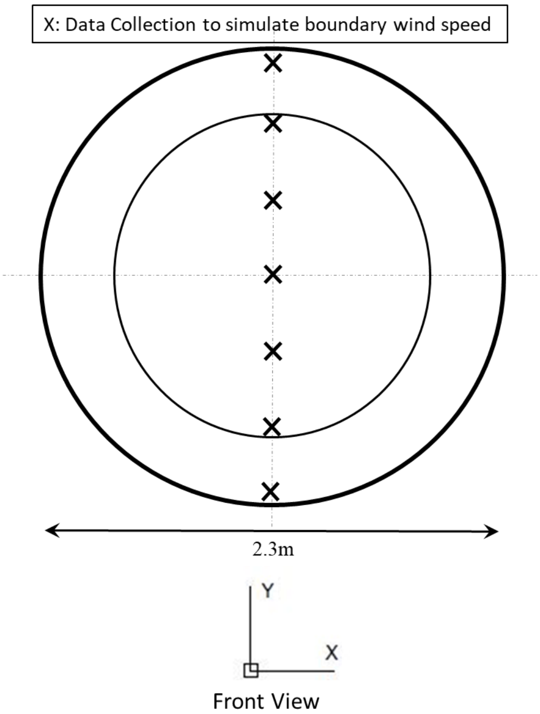

Fig. 8. Point wind speed at the wind tunnel opening centerline on the y-axis with maximum wind tunnel motor frequency (Hz)

Figure 9 to 12 show the turbulence intensity obtained at 53 distribution positions for every layer of Position 1 to Position 4, respectively. The turbulence intensity is obtained by calculating the average wind speed divided by standard deviation at each distribution points. Eq. (1) is used to obtain turbulence intensity, TI_i, where σ_i is the average of wind speed, and U_{mean} is the standard deviation of σ_i.

$$TI_i = \frac{\sigma_i}{U_{mean}} \times 100\% \quad (1)$$

The highest turbulence intensity at Position 1 is 27.7 % which is measured at the top side of the wind outlet shown in Figure 9. This indicates the top side has high turbulence compared to other areas. Meanwhile, at Position 2, the highest turbulence intensity is 25.8 % which is at the left side of the area, as shown in Figure 10.

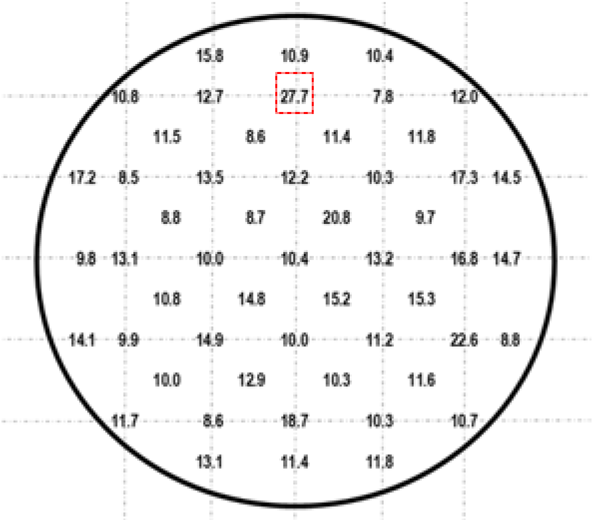

Fig. 9. Turbulence Intensity (%) at Position 1

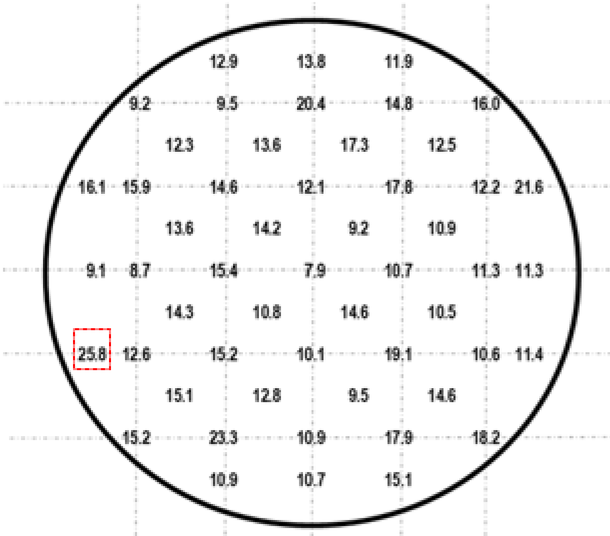

Fig. 10. Turbulence Intensity (%) at Position 2

However, several areas at Position 3 shows high turbulence intensity, which can be seen from Figure 11. The turbulence intensity observed at Position 3 is the highest turbulence intensity at 29.9 % located in the lower section, as shown by the dotted box. The measured data also indicate that higher turbulence areas are located at the upper and lower left-hand side with 26.2 % and 26.9 % respectively.

Lastly, at Position 4, the highest turbulence intensity recorded is 28 %, as shown in Figure 12. It also shows that the area with higher turbulence intensity is located more randomly with the highest reading near the center of the outlet.

The average turbulence intensity obtained at every distribution point for Position 1,2,3 and 4 is averaged as in Table 3. Data shows that wind speed decreased, and average turbulence intensity slightly decrease at Position 2. At Position 3, the turbulence intensity increases (see Figure 13).

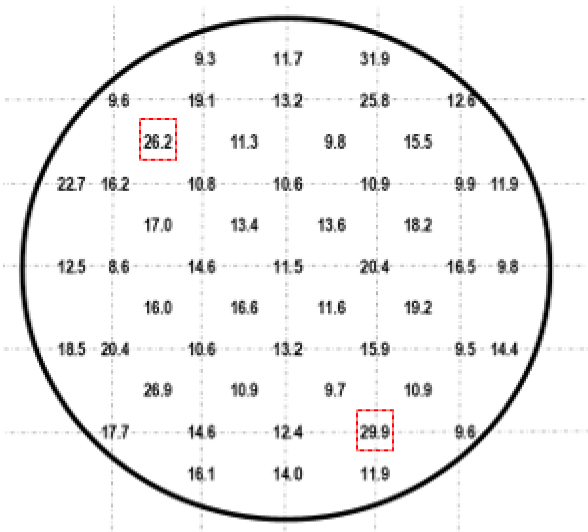

Fig. 11. Turbulence Intensity (%) at Position 3

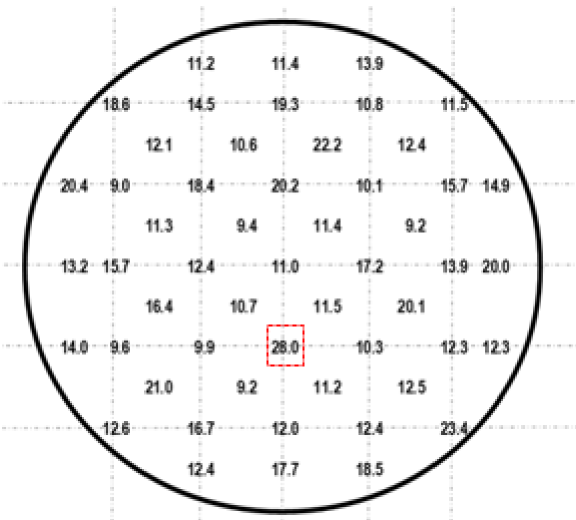

Fig. 12. Turbulence Intensity (%) at Position 4

Table 3
Open-jet wind tunnel wind speed by section in maximum wind tunnel hertz

Position	Wind speed average (m/s)	Standard deviation	Turbulence Intensity (%)
1	8.90	2.44	27.35

2	7.42	1.95	26.26
3	6.87	2.29	34.87
4	6.21	2.20	35.41

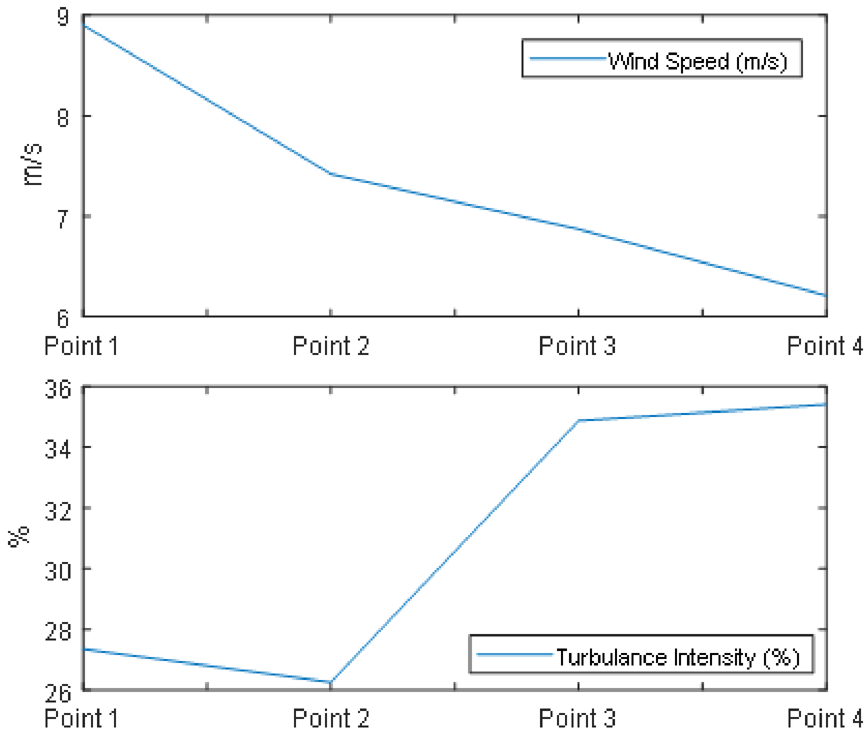

Fig. 13. Open-jet wind tunnel wind speed versus Turbulence Intensity at Position 1, 2,3 and 4

The data collected for the open-jet wind tunnel is compared to the wind speed distribution before the attachment of the diffuser at the open-loop wind tunnel outlet. Figure 14 shows the turbulence intensity versus wind speed at the exit of the wind tunnel before and after attachment of diffuser, settling chamber, and flow condition controls.

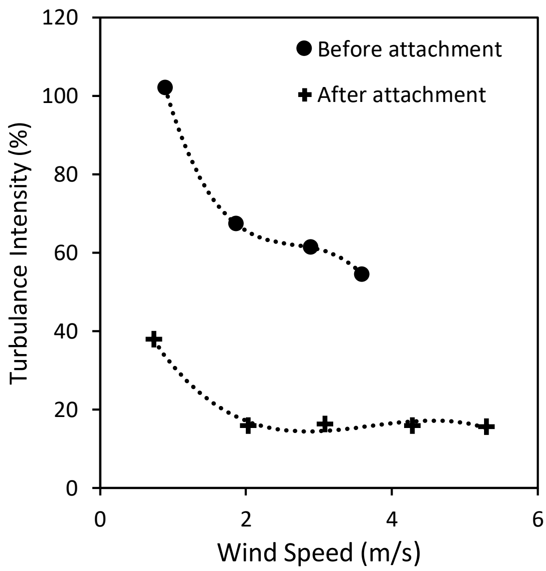

Fig. 14. Turbulence intensity comparison before and after improvement

From Figure 14, the attachment of the diffuser at the open-loop wind tunnel outlet has significantly reduced the turbulence intensity from around 60 % to around 20 %. Before attachment, the exit of open-loop wind tunnel produced high turbulence intensity due to the swirl effect of wind flow. This steep drop is contributed by the open-jet wind tunnel flow condition control device, which consists of mesh wire and honeycomb. The turbulence intensity of around 20 % can represent and simulate wind speed condition at the height of below 100m as shown by Tabrizi *et al.,* [14] and Carpman [13], which would be sufficient for the test flight of our quadrotor.

4. Conclusions

The finding shows that the feasibility of the open-jet tunnel used to test the hovering quadrotor in terms of outlet wind characteristics. The extended wind tunnel's flow characteristics are analyzed by the anemometer for velocity distribution in four different distance from the opening. It has been found that the wind velocity distribution and turbulent intensity simulate the local outdoor wind turbulent condition to test a quadrotor hovering control algorithm.

Acknowledgment
The research was supported by the Fundamental Research Grant Scheme, FRGS (grant no: FRGS/1/2015/TK09/UPM/02/4) and (grant no: FRGS/1/2018/TK09/UPNM/03/3). The authors are thankful to Mr. Saffairus Salih for equipment setups and participation during the duration of testing.

References
[1] Perozzi, Gabriele, Denis Efimov, Jean-Marc Biannic, Laurent Planckaert, and Patricia Coton. "Wind estimation algorithm for quadrotors using detailed aerodynamic coefficients." In *2018 Annual American Control Conference (ACC)*, pp. 1921-1926. IEEE, 2018.
[2] Ke, Yijie, Kangli Wang, Kehong Gong, Shupeng Lai, and Ben M. Chen. "Model based robust forward transition control for tail-sitter hybrid unmanned aerial vehicles." In *2017 13th IEEE International Conference on Control & Automation (ICCA)*, pp. 828-833. IEEE, 2017.
[3] Joyo, M. Kamran, D. Hazry, S. Faiz Ahmed, M. Hassan Tanveer, Faizan A. Warsi, and A. T. Hussain. "Altitude and horizontal motion control of quadrotor UAV in the presence of air turbulence." In *2013 IEEE Conference on Systems, Process & Control (ICSPC)*, pp. 16-20. IEEE, 2013.
[4] Waslander, Steven, and Carlos Wang. "Wind disturbance estimation and rejection for quadrotor position control." In *AIAA Infotech@ Aerospace conference and AIAA unmanned... Unlimited conference*, p. 1983. 2009.
[5] Bannwarth, J. X. J., Z. J. Chen, K. A. Stol, and B. A. MacDonald. "Disturbance accomodation control for wind rejection of a quadcopter." In *2016 International Conference on Unmanned Aircraft Systems (ICUAS)*, pp. 695-701. IEEE, 2016.
[6] Nor, E. Mohd, S. B. Noor, M. R. Bahiki, and S. Azrad. "Implementation of high-gain observer on low-cost fused IR-OS sensor embedded in UAV system." In *Materials Science and Engineering Conference Series*, vol. 270, no. 1, p. 012020. 2017.
[7] MN, Elya, S. B. Noor, Ribhan Zafira AR, and Syaril Azrad. "Application of Sliding Mode Control with Extended High Gain Observer to Stabilize the Underactuated Quadrotor System." *Pertanika Journal of Science & Technology* 25, no. S (2017): 343–352.
[8] Zain, Nadhirah Mohd, Shabudin Mat, Khushairi Amri Kasim, Shuhaimi Mansor, Md Nizam, and Norazila Othman Dahalan. "Wind tunnel experiments on a generic sharp-edge delta wing UAV Model." *Journal of Advanced Research in Fluid Mechanics and Thermal Science* 40, no. 1 (2017): 18-26.
[9] Bannwarth, J. X. J., Z. J. Chen, Karl A. Stol, Bruce A. MacDonald, and P. J. Richards. "Development of a Wind Tunnel Experimental Setup for Testing Multirotor Unmanned Aerial Vehicles in Turbulent Conditions." In *2018 IEEE/ASME International Conference on Advanced Intelligent Mechatronics (AIM)*, pp. 724-729. IEEE, 2018.

[10] Kamarudin, Muhammad Nizam, Abdul Rashid Husain, Mohamad Noh Ahmad, and Zaharuddin Mohamed. "Model and Analysis of Wind Speed Profile using Artificial Neural Network-Feasibility Study in Peninsular Malaysia." *Jurnal Teknologi* 74, no. 1 (2015): 77-80.
[11] Ahmadian, J., M. J. Ghorbanian, S. Shams, F. Goodarzvand, and J. Selvaraj. "Butterworth, Malaysia wind energy potential assessment." In *2013 IEEE Conference on Clean Energy and Technology (CEAT)*, pp. 13-18. IEEE, 2013.
[12] Ren, Guorui, Jinfu Liu, Jie Wan, Fei Li, Yufeng Guo, and Daren Yu. "The analysis of turbulence intensity based on wind speed data in onshore wind farms." *Renewable energy* 123 (2018): 756-766.
[13] Carpman, Nicole. "Turbulence intensity in complex environments and its influence on small wind turbines." (Master thesis, Uppsala University, 2011).
[14] Tabrizi, Amir Bashirzadeh, Jonathan Whale, Thomas Lyons, and Tania Urmee. "Rooftop wind monitoring campaigns for small wind turbine applications: Effect of sampling rate and averaging period." *Renewable energy* 77 (2015): 320-330.
[15] Yazid, AW Muhammad, CS Nor Azwadi, S. Mohamed Salim, and S. Mansor. "Preliminary Study on the Wind Flow and Pollutant Dispersion in an Idealized Street Canyon." *Journal of Advanced Research Design* 1, no. 1 (2014): 1-17.
[16] Vita, Giulio, Hassan Hemida, Thomas Andrianne, and Charalampos C. Baniotopoulos. "Generating atmospheric turbulence using passive grids in an expansion test section of a wind tunnel." *Journal of Wind Engineering and Industrial Aerodynamics* 178 (2018): 91-104.
[17] Ahmadi-Baloutaki, Mojtaba, Rupp Carriveau, and David S-K. Ting. "Performance of a vertical axis wind turbine in grid generated turbulence." *Sustainable Energy Technologies and Assessments* 11 (2015): 178-185.
[18] Azzawi, Itimad DJ, X. Mao, and Artur J. Jaworski. "Design, Fabrication and Characterization of Low Speed Open-jet Wind Tunnel." In *Proceeings of World Congress on Engineering 2016*, vol. 2, pp. 883-888. Newswood Limited, 2016.
[19] Sabikan, S., and S. W. Nawawi. "Open-source project (OSPs) platform for outdoor quadcopter." *Journal of Advanced Research Design* 24, no. 1 (2016): 13-27.
[20] Wiriadidjaja, Surjatin, Fadilah Hasim, Shuhaimi Mansor, Waqar Asrar, Azmin Shakrine Mohd Rafie, and Ermira Junita Abdullah. "Subsonic wind tunnels in Malaysia: a Review." In *Applied Mechanics and Materials*, vol. 225, pp. 566-571. Trans Tech Publications, 2012.